

Gene *bb0318* Is Critical for the Oxidative Stress Response and Infectivity of *Borrelia burgdorferi*

Adrienne C. Showman, George Aranjuez, Philip P. Adams,  Mollie W. Jewett

Division of Immunity and Pathogenesis, Burnett School of Biomedical Sciences, University of Central Florida College of Medicine, Orlando, Florida, USA

A greater understanding of the molecular mechanisms that *Borrelia burgdorferi* uses to survive during mammalian infection is critical for the development of novel diagnostic and therapeutic tools to improve the clinical management of Lyme disease. By use of an *in vivo* expression technology (IVET)-based approach to identify *B. burgdorferi* genes expressed *in vivo*, we discovered the *bb0318* gene, which is thought to encode the ATPase component of a putative riboflavin ABC transport system. Riboflavin is a critical metabolite enabling all organisms to maintain redox homeostasis. *B. burgdorferi* appears to lack the metabolic capacity for *de novo* synthesis of riboflavin and so likely relies on scavenging riboflavin from the host environment. In this study, we sought to investigate the role of *bb0318* in *B. burgdorferi* pathogenesis. No *in vitro* growth defect was observed for the Δ *bb0318* clone. However, the mutant spirochetes displayed reduced levels of survival when exposed to exogenous hydrogen peroxide or murine macrophages. Spirochetes lacking *bb0318* were found to have a 100-fold-higher 50% infectious dose than spirochetes containing *bb0318*. In addition, at a high inoculum dose, *bb0318* was found to be important for effective spirochete dissemination to deep tissues for as long as 3 weeks postinoculation and to be critical for *B. burgdorferi* infection of mouse hearts. Together, these data implicate *bb0318* in the oxidative stress response of *B. burgdorferi* and indicate the contribution of *bb0318* to *B. burgdorferi* mammalian infectivity.

Borrelia burgdorferi, the causative agent of Lyme disease, is an obligate pathogen, relying on both its tick vector and its mammalian host for many of its nutrients. With a genome of only 1.5 Mbp, *B. burgdorferi* has significantly limited metabolic and biosynthetic capabilities, lacking genes encoding enzymes for *de novo* synthesis of amino acids, nucleotides, vitamin cofactors, and fatty acids (1–3). Thus, *B. burgdorferi* maintains a host-dependent lifestyle, acquiring these metabolic and biosynthetic precursors from its host environments. The genome of *B. burgdorferi* contains at least 52 open reading frames (ORFs) that encode transport and binding proteins, for a recognized 37 transport systems (1, 4). The utilization of transport systems to obtain biomolecules as precursors for essential metabolic processes is likely critical to the survival of *B. burgdorferi* throughout its infectious life cycle. Indeed, a subset of *B. burgdorferi* nutrient uptake systems has been demonstrated to play important roles in spirochete survival *in vivo* (5–8). This finding, as well as the fact that this spirochete lacks classical virulence factors, suggests that the ability of *B. burgdorferi* to scavenge nutrients and metabolites is not only a survival mechanism but also a significant component of *B. burgdorferi* pathogenesis. This ability therefore presents a possible avenue for the development of novel therapeutics for Lyme disease.

B. burgdorferi experiences deleterious reactive oxygen species (ROS) throughout its enzootic cycle. In contrast to the mechanism for most bacteria, DNA is not the major target of ROS damage in *B. burgdorferi*, likely due to the lack of intracellular free iron to generate the harmful effects of the Fenton reaction (9, 10). Rather, the unsaturated fatty acids contained in the *B. burgdorferi* membranes have been shown to be a primary target of ROS, resulting in lipid peroxidation and a loss of membrane integrity (9).

The oxidative stress response is critical for *B. burgdorferi* pathogenesis (11–17). BosR is a transcriptional regulator (12, 17–24) that is required for optimal resistance to oxidative stress (25) and the production of oxidative stress proteins, including superoxide dismutase (SodA) and coenzyme A disulfide reductase (CoADR,

encoded by the *cdr* gene) (12, 14, 17, 18, 24–26). Spirochetes lacking *bosR*, *sodA*, or *cdr* are avirulent in mice (13, 14, 19, 20, 25). Studies on the role of SodA during infection have demonstrated that this protein is important for controlling the levels of oxidation of critical metabolic proteins, as well as the production of factors known to be critical for infection (27).

Our application of an *in vivo* expression technology (IVET)-based genetic screen to seek out transcriptionally active regions of the *B. burgdorferi* genome during murine infection identified the candidate *in vivo*-expressed gene *bb0318* (28), which is annotated to encode the ATP-binding protein of an ABC-type sugar transport system (1). The *bb0318* gene is located within a putative operon including genes *bb0319* to *bb0316* (1, 29) and possibly *bb0321* and *bb0322* (30, 31). Genes *bb0319* to *bb0316*, but not *bb0321* and *bb0322*, are conserved in *Treponema pallidum* and *Treponema denticola*, and the homologs have been shown to be cotranscribed in *T. pallidum* (29). Furthermore, purified, recombinant BB0319, TP0298, and TDE0951, the putative substrate binding proteins from the *B. burgdorferi*, *T. pallidum*, and *T. denticola* transport systems, respectively, have been demonstrated to bind riboflavin. These data suggest that genes *bb0319* to *bb0316*

Received 20 May 2016 Returned for modification 14 June 2016

Accepted 8 August 2016

Accepted manuscript posted online 22 August 2016

Citation Showman AC, Aranjuez G, Adams PP, Jewett MW. 2016. Gene *bb0318* is critical for the oxidative stress response and infectivity of *Borrelia burgdorferi*. *Infect Immun* 84:3141–3151. doi:10.1128/IAI.00430-16.

Editor: C. R. Roy, Yale University School of Medicine

Address correspondence to Mollie W. Jewett, Mollie.Jewett@ucf.edu.

Supplemental material for this article may be found at <http://dx.doi.org/10.1128/IAI.00430-16>.

Copyright © 2016, American Society for Microbiology. All Rights Reserved.

may encode a ligand binding-dependent ABC transport system for riboflavin uptake (29).

Riboflavin is the precursor molecule required for synthesis of the enzyme cofactors flavin mononucleotide (FMN) and flavin adenine dinucleotide (FAD) (32). The *B. burgdorferi* genome appears to lack the genes encoding the typical enzymes involved in the synthesis of riboflavin, FMN, and FAD (1). However, the concentration of FAD within *B. burgdorferi* has been found to be approximately 1 μM (33), and *B. burgdorferi* has putative flavoenzymes (13, 26), suggesting that the spirochete may possess mechanisms to transport and/or synthesize FMN and FAD. For instance, BB0812 is a putative flavoenzyme, annotated as a bifunctional phosphopantothencysteine decarboxylase/phosphopantothenate-cysteine ligase involved in coenzyme A (CoA) biosynthesis (1, 34), and FAD is a predicted cofactor for *B. burgdorferi* CoADR (11, 13). Unlike *Escherichia coli*, which uses the low-molecular-weight thiol glutathione and glutathione reductase (GSH/Gor), *B. burgdorferi* does not produce GSH and lacks a Gor homolog (1, 11). Instead, *B. burgdorferi* produces the low-molecular-weight thiol CoA, and the CoA/CoADR redox system is predicted to serve as an important pathway for eliminating ROS in the spirochete (11, 13, 33). Moreover, not only has CoADR been proposed to contribute to thiol/disulfide homeostasis and intermediary metabolism (13), but the flavoenzyme has also been shown to be critical for *B. burgdorferi* resistance to oxidative stress and its survival in the enzootic cycle (13). The putative riboflavin transport system, encoded by *bb0319* to *bb0316*, may therefore aid in the ability of *B. burgdorferi* to resist oxidative stress and to combat the host innate immune response during infection, as the first step in the synthesis of a cofactor critical to its low-molecular-weight thiol redox system.

To elucidate the role of *bb0318* during murine infectivity, we generated a *B. burgdorferi* in-frame deletion mutant lacking this gene. We demonstrate that Δbb0318 mutant spirochetes have increased sensitivity to hydrogen peroxide and murine macrophages *in vitro*, are highly attenuated in their ability to infect mice, and fail to exhibit detectable bacterial loads in murine heart tissue. Together, these findings indicate that *bb0318* is important for *B. burgdorferi* infection of the mammalian host and suggest that the proposed nutrient uptake function of the BB0319-to-BB0316 ABC transport system is critical for *B. burgdorferi* pathogenesis.

MATERIALS AND METHODS

Bacterial clones and growth conditions. All *B. burgdorferi* clones were derived from the low-passage-number infectious clone B31 A3. B31 A3-68 Δbbe02 lacks plasmids cp9 and lp56, as well as the *bbe02* gene on lp25 (35). *B. burgdorferi* cultures were grown in liquid Barbour-Stoenner-Kelly II (BSKII) medium containing gelatin and 6% rabbit serum at 35°C. Individual colonies were isolated by plating on solid BSK medium as described previously (36, 37) and were grown at 35°C under 2.5% CO₂. *B. burgdorferi* cultures were grown in the presence of kanamycin (200 $\mu\text{g}/\text{ml}$), streptomycin (50 $\mu\text{g}/\text{ml}$), and/or gentamicin (40 $\mu\text{g}/\text{ml}$), as appropriate. Cloning steps were performed using *Escherichia coli* DH5 α , grown in lysogeny broth (LB) or on LB agar plates. For *E. coli* cultures, kanamycin was used in at 50 $\mu\text{g}/\text{ml}$, spectinomycin at 300 $\mu\text{g}/\text{ml}$, and/or gentamicin at 10 $\mu\text{g}/\text{ml}$, as appropriate.

Generation of an in-frame deletion of *bb0318* and the genetic complement. The *bb0318* deletion construct was engineered for in-frame replacement of the *bb0318* open reading frame with the promoterless spectinomycin/streptomycin resistance gene *aadA* by the PCR-based overlap extension strategy described previously (28) using primers 1825, 1826,

and 2084 to 2087 (Table 1). The allelic exchange plasmid pCR-BLUNT- Δbb0318 -*aadA* was verified by PCR, restriction enzyme digestion, and DNA sequence analysis. *B. burgdorferi* A3-68 Δbbe02 was transformed with 20 μg of pCR-Blunt- Δbb0318 -*aadA* purified from *E. coli* as described previously (38). Streptomycin-resistant colonies were confirmed to be true transformants by PCR using primer pairs 1825–1826 and 2084–2085 (Table 1). Positive Δbb0318 -*aadA* clones were screened with a panel of primers (39) for the presence of all of the *B. burgdorferi* plasmids of the parent A3-68 Δbbe02 clone (35), and a single clone was selected for further experiments.

The Δbb0318 clone was complemented in *trans* using the *B. burgdorferi* shuttle vector pBSV2G (40). A DNA fragment containing the *bb0318* gene and an additional 362 bp of upstream sequence containing the putative endogenous promoter was amplified from B31 A3 genomic DNA using the Phusion enzyme (Thermo Scientific) and primers 2088 and 2089. When amplified, these primers introduced a KpnI restriction enzyme site at the 5' end, and a SalI site at the 3' end, of the PCR product. Following digestion with KpnI and SalI, pBSV2G was ligated with the DNA fragment and transformed into *E. coli*. The pBSV2G *bb0318* plasmid structure and the presence of the DNA fragment were verified by PCR, restriction enzyme digestion, and DNA sequence analysis. Δbb0318 -*aadA* spirochetes were then transformed with 20 μg pBSV2G *bb0318* or pBSV2G alone, and positive transformants were selected as described previously (38). The clones that retained the *B. burgdorferi* plasmid content of the parent clone were selected for use in further experiments.

In vitro growth analysis. Wild-type (A3-68 ΔBBE02), $\Delta\text{bb0318}/\text{pBSV2G}$, and $\Delta\text{bb0318}/\text{pBSV2G}$ *bb0318* spirochetes were inoculated in triplicate cultures at a starting density of 1×10^5 spirochetes/ml in 5 ml of BSKII medium containing the appropriate antibiotics. Spirochete densities were determined every 24 h by cell enumeration under dark-field microscopy using a Petroff-Hausser chamber over a 144-h period.

RNA isolation. Biological triplicate cultures of wild-type (A3-68 Δbbe02), $\Delta\text{bb0318}/\text{pBSV2G}$, and $\Delta\text{bb0318}/\text{pBSV2G}$ *bb0318* spirochetes were grown to log phase (3×10^7 to 6×10^7 cells/ml) in 45 ml of BSKII medium. Cells were pelleted by centrifugation at $3,210 \times g$ for 15 min. Pellets were snap-frozen in liquid nitrogen and resuspended in 640 μl of TE buffer (10 mM Tris, 1 mM EDTA [pH 8]) containing 0.5 mg/ml lysozyme and 1% SDS. RNA was isolated by hot phenol-chloroform extraction and ethanol precipitation as described previously (41). Samples were resuspended in diethyl pyrocarbonate (DEPC)-treated distilled water (dH₂O). Contaminating DNA was removed using recombinant DNase I (Roche) in a 50- μl reaction mixture containing as much as 50 μg of RNA, 10 U of DNase I, ~ 60 U of recombinant rRNasin (Promega), and 5 μl of 10 \times incubation buffer (Roche), incubated at 37°C for 15 min. DNase I treatment was followed by phenol-chloroform extraction and ethanol precipitation as described above.

Gene expression analysis. cDNA was synthesized from 500 ng of RNA isolated from *in vitro*-grown spirochetes using the iScript Select cDNA synthesis kit and random hexamers (Bio-Rad), according to the manufacturer's instructions. Parallel cDNA reactions were carried out in the absence of reverse transcriptase (RT). One hundred nanograms of cDNA was used as the template in subsequent real-time quantitative PCRs (qPCRs). qPCR was performed using iQ SYBR green supermix and the following primer pairs: 1202 and 1203 (*bb0319*), 1230 and 1231 (*bb0318*), 1196 and 1197 (*bb0317*), 1192 and 1193 (*bb0316*), and 1123 and 1124 (*recA*). The amounts of *bb0319*, *bb0318*, *bb0317*, *bb0316*, and *recA* transcripts were determined using a genomic DNA standard curve for each gene target with 10 ng, 1 ng, 0.1 ng, and 0.01 ng of DNA. Both standard-curve reactions and PCRs using cDNA for each biological triplicate were performed in technical triplicate. mRNA transcript copy numbers for *bb0319*, *bb0318*, *bb0317*, and *bb0316* were normalized to *recA* copies. All data sets were compared using one-way analysis of variance (ANOVA) followed by Tukey's posttest (GraphPad Prism, version 6.0).

H₂O₂ susceptibility assays. Wild-type (A3-68 Δbbe02), $\Delta\text{bb0318}/\text{pBSV2G}$, and $\Delta\text{bb0318}/\text{pBSV2G}$ *bb0318* clones were grown to mid-log

TABLE 1 Primers and probes used in this study

Primer or probe no.	Designation	Sequence (5'–3') ^a
Primers		
2084	BB0318 +500 5'	TATTGCTTAATATTTCAAGCTGAAGACC
2085	BB0318 –500 3'	TAAATCTGGCTTTGGAAATGCTG
1825	<i>aadA</i> 5' FWD	ATGAGGGAAGCGGTGATCGCCGAAG
1826	<i>aadA</i> 3' RVS	TTATTTGCCGACTACCTTGGTGATCTGCCTT
2086	BB0318 +500 3' in frame	GGCGAGATCACCAAGGTAGTCGGCAAATGATCTTTTTTAGAAATAGCTTTATG
2087	BB0318 –500 5' in frame	CTTCGGCGATCACCGCTTCCTCATTAAATTTGTTCCAAATTAATTTTATACC
2088	BB0318 comp fwd KpnI	GGTACCGCTTTGGTAATACTTCCTATTG
2089	BB0318 comp rvs Sall	GTCGACTCATAAAAAATAGCAATTCCTTTAATTTTTTC
1230	BB0318 FWD qPCR assay	CAGATATTGACAAGCCTATTG
1231	BB0318 REV qPCR assay	CCTCATCAAATTCATAAGTCC
1123	<i>recA</i> FWD	AATAAGGATGAGGATTGGTG
1124	<i>recA</i> RVS	GAACCTCAAGTCTAAGAGATG
1202	BB0319 inter 5'	CCGGGAATAAAATAAGCAATATTG
1203	BB0319 inter 3'	AGGGTTTTGGATTTTATTACG
1196	BB0317 inter 5'	CTAAAAATGCCCAAATAAATCTG
1197	BB0317 inter 3'	TTATATTAATAATGATATCTTGGCGC
1192	BB0316 inter 5'	CGTTGATTAAGAGAAAAGATAGATC
1193	BB0316 inter 3'	GTTGACATAAAAAATCCATATCCC
1137	<i>flaB</i> -TaqMan-FWD	TCTTTTCTCTGGTGAGGGAGCT
1138	<i>flaB</i> -TaqMan-REV	TCCTTCCTGTTGAACACCCTCT
1140	<i>nid</i> -TaqMan-FWD	CACCCAGCTTCGGCTCAGTA
1141	<i>nid</i> -TaqMan-REV	TCCCCAGGCCATCGGT
1037	pUC18F	CCCAGTCACGACGTTGTAAAAC
1668	pUC18R	AGCGGATAACAATTCACACAG
Probes		
1139	<i>flaB</i> -TaqMan-Probe	6-FAM-AAACTGCTCAGGCTGCACCGGTTT-CAMRA
1142	<i>nid</i> -TaqMan-Probe	6-FAM-CGCCTTCTCTGGCTGACTTGGACA-TAMRA

^a 6-FAM, 6-carboxyfluorescein; TAMRA, 6-carboxytetramethylrhodamine.

phase (5×10^7 spirochetes/ml) in BSKII medium with the appropriate antibiotics. The spirochetes were washed twice in HN buffer (50 mM HEPES, 50 mM NaCl [pH 7.6]) and were resuspended in modified BSKII medium without sodium pyruvate (42) to a density of 1×10^4 spirochetes/ml. Reaction mixtures containing 1×10^4 spirochetes and either no hydrogen peroxide or 10 mM, 15 mM, or 20 mM hydrogen peroxide were incubated for 2 h at 35°C under 2.5% CO₂. Serial dilutions were plated for CFU on solid BSK plating medium (36, 37). The percentage of survival was calculated by dividing the CFU under each H₂O₂ condition by the CFU in the absence of H₂O₂ and multiplying by 100. All experiments were performed at least three times. All data sets were compared using one-way ANOVA followed by Tukey's posttest (GraphPad Prism, version 6.0).

Macrophage killing assays. Mouse-derived J774 macrophages were grown in Dulbecco's modified Eagle medium (DMEM) (Gibco) supplemented with 10% fetal bovine serum (FBS) (Atlanta Biologicals) and 2 mM L-glutamine (Gibco) at 37°C under 5% CO₂. Approximately 5×10^3 macrophages were seeded in 96-well tissue culture plates and were allowed to settle and attach for 24 h. Wild-type (A3-68Δ*bbe02*), Δ*bb0318*/pBSV2G, and Δ*bb0318*/pBSV2G *bb0318* clones were grown to mid-log phase (5×10^7 spirochetes/ml) in BSKII medium with the appropriate antibiotics. A total of 5×10^4 spirochetes per clone were added to wells containing 100 μl of DMEM plus FBS and L-glutamine with or without preseeded J774 macrophages. The plates were gently centrifuged at $50 \times g$ for 5 min and were incubated at 37°C under 5% CO₂ for 4 h (14). *B. burgdorferi* CFU counts were determined by plating the sample supernatants on solid BSK medium. The percentage of survival for each clone was calculated by dividing the CFU in the presence of macrophages by the CFU in medium alone and multiplying by 100. All experiments were performed in at least biological triplicate. All data sets were compared

using one-way ANOVA followed by Tukey's posttest (GraphPad Prism, version 6.0).

Mouse infection experiments. The University of Central Florida (UCF) is accredited by the International Association for Assessment and Accreditation of Laboratory Animal Care, and all experiments were approved by the Institutional Animal Care and Use Committee of UCF. All spirochetes used for mouse infection studies were grown to the same stationary-phase density ($\sim 1 \times 10^8$ /ml) in BSKII medium and were then diluted to the desired inoculum density just prior to use. All inoculum densities were determined using a Petroff-Hausser counting chamber and were verified by CFU counts on solid BSK medium. All inoculum cultures were analyzed for the endogenous plasmid content by PCR, and individual colonies from each population were analyzed for the presence of virulence plasmids lp25, lp28-1, and lp36 (43). All inoculum cultures carried the expected endogenous plasmid content, and 80 to 100% of individual colonies from each clone were confirmed to contain all three virulence plasmids. For the 50% infectious dose (ID₅₀) analysis, groups of six 6- to 8-week-old female C3H/HeN mice (Envigo) were needle inoculated intraperitoneally (80% dose) and subcutaneously (20% dose) with 10-fold increasing doses as follows: A3-68Δ*bbe02* (wild-type), 1×10^3 to 1×10^5 spirochetes; Δ*bb0318*/pBSV2G, 1×10^4 to 1×10^7 spirochetes; Δ*bb0318*/pBSV2G *bb0318*, 1×10^3 to 1×10^5 spirochetes. The 50% infectious dose for each clone and associated 90% confidence intervals were calculated using probit regression analysis (JMP, version 12.2.0; SAS Institute, Inc.). For single-dose infection studies, groups of six 6- to 8-week-old female C3H/HeN mice (Envigo) were needle inoculated intraperitoneally (80%) and subcutaneously (20%) with 1×10^7 A3-68Δ*bbe02* (wild-type), Δ*bb0318*/pBSV2G, or Δ*bb0318*/pBSV2G *bb0318* spirochetes. Unless specified otherwise, mouse infection was assessed 3 weeks postinoculation by serology and/or reisolation of spirochetes from ear, bladder, and joint

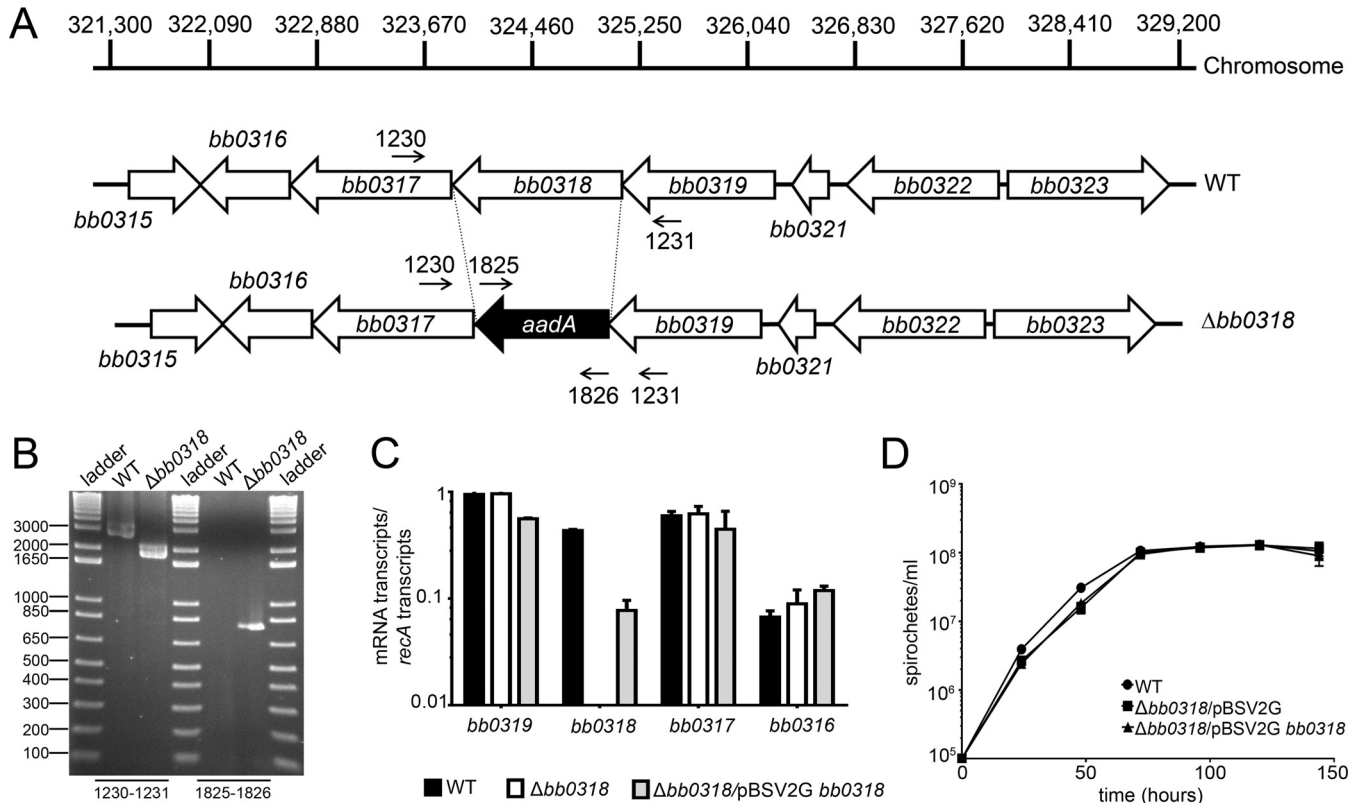


FIG 1 The in-frame deletion of *bb0318* is nonpolar and has no effect on spirochete growth *in vitro*. (A) Schematic representation of the wild-type (WT) and $\Delta bb0318$ loci on the chromosome. The sequence of the BB0318 open reading frame was replaced directly in frame with the *aadA* antibiotic resistance cassette in order to prevent a polar effect on the expression of the surrounding genes. Dashed lines mark deletion boundaries; primer numbers and small arrows indicate the locations of primers used to verify the mutant construct. (B) PCR analysis of the *bb0318* mutant clone. Genomic DNAs from WT-background spirochetes and $\Delta bb0318$ spirochetes were used as the templates for PCR analyses (indicated above the gel). The primer pairs used to amplify specific DNA sequences correspond to the labels in panel A and are given beneath the gel. DNA ladder fragment sizes (in base pairs) are given on the left. (C) qRT-PCR analysis of genes surrounding *bb0318* in mutant and complemented clones. Spirochete RNA was isolated from log-phase-grown WT, mutant, and complemented clones, and the expression of the *recA*, *bb0319*, *bb0318*, *bb0317*, and *bb0316* genes was quantified by reverse transcriptase qPCR. The data are expressed as the number of mRNA transcripts per number of *recA* transcripts and are averages for three biological replicates. (D) Analysis of the growth of WT, $\Delta bb0318/pBSV2G$, and $\Delta bb0318/pBSV2G bb0318$ spirochetes. Clones were grown in 5-ml biological triplicate cultures and were enumerated by dark-field microscopy every 24 h.

tissues, as described previously (6). A mouse was considered infected if spirochetes were reisolated from at least one of the three tissues analyzed.

Quantification of spirochete loads in mouse tissues. Ear, heart, and joint tissues were collected from mice 1, 2, or 3 weeks after inoculation with *B. burgdorferi*, and DNA was extracted as described previously (44). Spirochete loads in mouse tissues were then determined by qPCR and a standard-curve approach as described above, using 100 ng of DNA extracted from mouse tissues as the template. The number of *B. burgdorferi* genomes was determined using *flaB* TaqMan primers and probe (primers 1137 and 1138; probe 1139), and the number of mouse genomes was determined using *nid* TaqMan primers and probe (primers 1140 and 1141; probe 1142). Each tissue sample was analyzed in triplicate qPCRs, and data are reported as the number of *flaB* copies per 10^{10} *nid* copies. All data sets were compared using one-way ANOVA followed by Tukey's posttest (GraphPad Prism, version 6.0).

RESULTS

Spirochetes lacking *bb0318* are not defective for *in vitro* growth. Gene *bb0318* is located on the *B. burgdorferi* chromosome within a predicted operon comprised of genes *bb0319* to *bb0316* (1, 29) and possibly *bb0321* and *bb0322* (30, 31). Genes *bb0319* to *bb0316* are tightly organized in the genome, with no nucleotides separating the adjacent open reading frames (1). Genes *bb0319* and *bb0321*

are separated by 180 bp, and genes *bb0321* and *bb0322* are separated by 32 bp (1). Genes *bb0321* and *bb0322* share no sequence identity with the genes upstream of the *bb0319*-to-*bb0316* homologs in *T. pallidum*. Gene *bb0318* was previously identified as a candidate gene expressed during murine infection (28). Quantitative reverse transcriptase PCR (qRT-PCR) analysis of RNA isolated from *B. burgdorferi*-infected unfed nymphs, fed nymphs, and mouse tissues indicated that the *bb0318* gene is expressed not only during murine infection but throughout the *B. burgdorferi* tick-mouse infectious cycle (see Fig. S1 in the supplemental material). Furthermore, the transcript levels detected for genes *bb0319*, *bb0318*, *bb0317*, and *bb0316* were distinct from one another within each of the three biologically relevant environments (Fig. S1). However, these data are unable to distinguish between differential expression of monocistronic transcripts and differential detection of each individual gene in a polycistronic operon due to RNA degradation.

To generate a *bb0318* mutant while avoiding polar effects on the surrounding genes, the entire BB0318 open reading frame was replaced in frame with the promoterless *aadA* spectinomycin/streptomycin resistance gene by allelic exchange in a low-passage-

number infectious derivative of *B. burgdorferi* strain B31 (Fig. 1A and B). Streptomycin-resistant clones lacking *bb0318* ($\Delta bb0318$) were successfully recovered on solid BSK medium containing streptomycin, demonstrating that the *aadA* gene was expressed within the *bb0319*-to-*bb0316* locus during *in vitro* growth. Complementation of *bb0318* was accomplished through reintroduction of *bb0318* along with 362 bp of additional upstream sequence on the *B. burgdorferi* shuttle vector pBSV2G (40) ($\Delta bb0318$ /pBSV2G *bb0318*). Analysis by qRT-PCR measuring the transcript levels of *bb0318* and the surrounding genes *bb0319*, *bb0317*, and *bb0316* in the wild-type, $\Delta bb0318$, and $\Delta bb0318$ /pBSV2G *bb0318* clones demonstrated that in-frame deletion of *bb0318* and its complementation in *trans* did not affect the expression of the adjacent genes (Fig. 1C). Expression of the *bb0318* gene was restored in the complemented clone, but to a level below that of the wild type (Fig. 1C), suggesting that additional upstream regulatory sequence may be necessary to drive wild-type levels of *bb0318* expression. However, *bb0318* expression in the $\Delta bb0318$ mutant harboring a *bb0318* complementation construct carrying 1,197 bp of upstream sequence, including *bb0318*, *bb0319*, and an additional 145 bp, demonstrated similar partial restoration (data not shown). Therefore, to avoid having both chromosomal and plasmid-encoded copies of *bb0319*, the $\Delta bb0318$ complement carrying only *bb0318* and 362 bp of upstream sequence was selected for use in subsequent experiments. *In vitro* growth analysis of wild-type, $\Delta bb0318$ /pBSV2G, and $\Delta bb0318$ /pBSV2G *bb0318* spirochetes showed no difference in growth over a 144-h period (Fig. 1D), indicating that *bb0318* is dispensable for spirochete growth in standard culture medium.

Spirochetes lacking *bb0318* are more susceptible to ROS-mediated killing. The BB0318 protein is the predicted ATPase component of a putative binding protein-dependent ABC transport system for riboflavin uptake (1, 29). Given that riboflavin is the precursor molecule for the synthesis of FMN and FAD, both of which are cofactors for flavoenzymes critical for the CoA/CoADR redox system, involved in resistance to oxidative stress (1, 11, 13, 26, 33), we hypothesized that $\Delta bb0318$ spirochetes might demonstrate increased susceptibility to reactive oxygen species (ROS). To test this hypothesis, the wild-type, $\Delta bb0318$ /pBSV2G, and $\Delta bb0318$ /pBSV2G *bb0318* clones were grown under standard conditions and were then treated with various concentrations of hydrogen peroxide (H_2O_2) ranging from 10 to 20 mM. Minimal killing of wild-type, $\Delta bb0318$ /pBSV2G, and $\Delta bb0318$ /pBSV2G *bb0318* spirochetes was observed at a dose of 10 mM H_2O_2 , with an average survival of approximately 80% for each clone (Fig. 2A). However, spirochetes lacking *bb0318* were significantly more susceptible than wild-type spirochetes to 15 mM or 20 mM exogenous H_2O_2 (Fig. 2A). Although not statistically significant, the trend in the data suggested greater susceptibility of the $\Delta bb0318$ /pBSV2G mutant than of the complemented clone to the 15 mM and 20 mM concentrations of H_2O_2 (Fig. 2A). There was no significant difference in susceptibility between the wild-type and *bb0318* complemented clones at 15 mM exogenous H_2O_2 ; however, treatment with 20 mM exogenous H_2O_2 resulted in significantly more killing of *bb0318* complemented spirochetes than of wild-type spirochetes.

To begin to understand the biological significance of the requirement for *bb0318* for wild-type levels of resistance to ROS, we analyzed the abilities of the wild-type, $\Delta bb0318$ /pBSV2G, and $\Delta bb0318$ /pBSV2G *bb0318* spirochetes to survive in the presence of

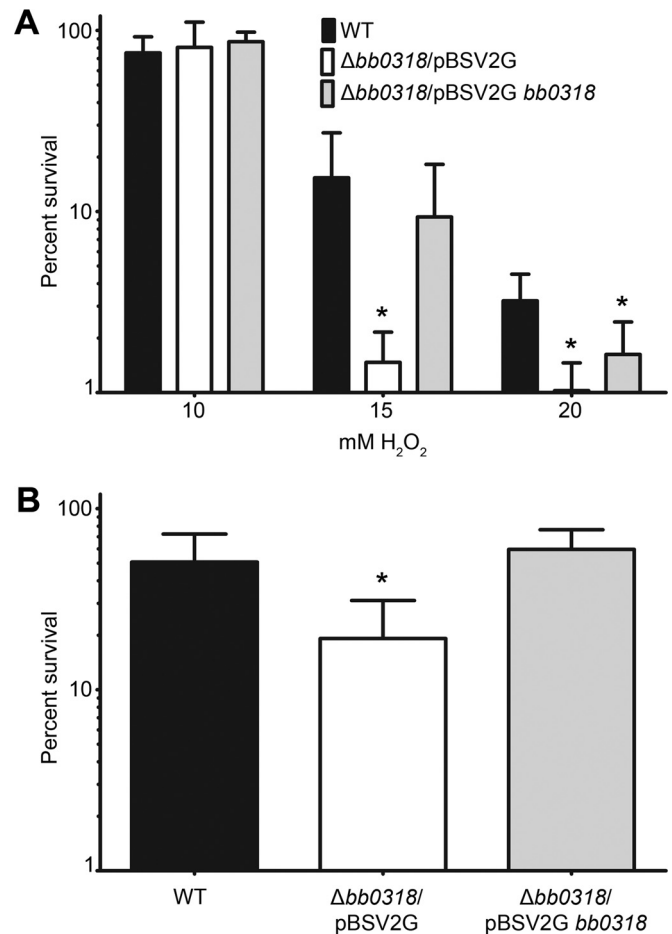


FIG 2 *bb0318* spirochetes demonstrate sensitivity to H_2O_2 and murine macrophages. (A) A total of 1×10^4 mid-log-phase wild-type (WT), $\Delta bb0318$ /pBSV2G, or $\Delta bb0318$ /pBSV2G *bb0318* spirochetes were either left unexposed or exposed to 10 mM, 15 mM, or 20 mM exogenous H_2O_2 . Following a 2-h incubation, spirochetes were serially diluted and were plated for CFU. (B) A total of 5×10^4 mid-log-phase WT, $\Delta bb0318$ /pBSV2G, or $\Delta bb0318$ /pBSV2G *bb0318* spirochetes were incubated in the presence or absence of J774 murine macrophages for 4 h. Spirochetes were serially diluted and were plated for CFU. The percentage of survival of each clone under each challenge condition was calculated by dividing the number of CFU in the presence of the challenge by the number of CFU for the matched medium-alone control, multiplying by 100, and subtracting from 100%. Data are averages \pm standard deviations for at least three biological replicates for each clone and are plotted on a logarithmic scale. Data sets were compared across clones by use of one-way ANOVA and Tukey's posttest (GraphPad Prism, version 6.0). Statistical comparisons were not found to be significant unless otherwise noted. Asterisks indicate significant differences ($P < 0.05$) from wild-type and/or $\Delta bb0318$ /pBSV2G *bb0318* spirochetes.

murine macrophages, one of the major sources of ROS produced by the innate immune system of the mammalian host in response to *B. burgdorferi* infection (45). In agreement with our findings of increased susceptibility to H_2O_2 , coinubation of spirochetes with murine macrophages resulted in a significantly lower percentage of survival of the $\Delta bb0318$ clone than of either the wild-type or the *bb0318* complemented clone (Fig. 2B). Together, these results indicate that in the absence of *bb0318*, the ability of *B. burgdorferi* to respond to ROS stress conditions is attenuated.

The infectious dose of spirochetes lacking *bb0318* is 100-fold greater than that of spirochetes containing *bb0318*. In order to

TABLE 2 Spirochetes lacking *bb0318* have a 100-fold-attenuated infectious dose

Clone genotype	No. of mice infected ^a /no. analyzed with the following spirochete dose:					ID ₅₀ (90% CI) ^c
	1 × 10 ³	1 × 10 ⁴	1 × 10 ⁵	1 × 10 ⁶	1 × 10 ⁷	
Wild type	0/6	1/6	3/6	N/A	N/A	3.6 × 10 ⁴ (7.9 × 10 ² –1.6 × 10 ⁶)
Δ <i>bb0318</i> /pBSV2G	N/A	0/6	0/6	1/6 ^b	5/6	3.5 × 10 ⁶ (1.0 × 10 ⁶ –1.2 × 10 ⁷)
Δ <i>bb0318</i> /pBSV2G <i>bb0318</i>	0/6	1/6	4/6	N/A	N/A	4.8 × 10 ⁴ (2.1 × 10 ³ –1.0 × 10 ⁶)

^a Mouse infection was determined 3 weeks postinoculation by positive reisolation of spirochetes from the ear, bladder, and joint tissues unless otherwise noted. N/A, not applicable.

^b Positive reisolation of spirochetes from bladder and joint tissues only.

^c The 50% infectious dose (ID₅₀) is the number of spirochetes required to infect 50% of the mice inoculated. The ID₅₀ values and associated 90% confidence intervals (90% CI) were calculated using probit regression analysis (JMP, version 12.2.0; SAS Institute, Inc.).

investigate the role of *bb0318* during a mammalian infection, we were interested in quantifying the infectious capability of *B. burgdorferi* with and without *bb0318*. In groups of six, C3H/HeN mice were needle inoculated with 10-fold increasing doses of wild-type, Δ*bb0318*/pBSV2G, or Δ*bb0318*/pBSV2G *bb0318* spirochetes. Three weeks postinoculation, the 50% infectious dose (ID₅₀) of each of these clones was determined on the basis of reisolation of spirochetes from ear, bladder, and joint tissues (Table 2). The ID₅₀ value for Δ*bb0318*/pBSV2G spirochetes was calculated by probit regression analysis to be 3.5 × 10⁶ spirochetes. This dose was approximately 100-fold greater than the ID₅₀ values calculated for the wild-type and Δ*bb0318*/pBSV2G *bb0318* spirochetes (3.6 × 10⁴ and 4.8 × 10⁴ spirochetes, respectively) (Fig. 3; Table 2). The ID₅₀ values for the wild-type and Δ*bb0318*/pBSV2G *bb0318* spirochetes identified in this experiment are slightly higher than those reported previously for the B31 A3 genetic background (28, 44, 46, 47). Together, these data suggest that *bb0318* promotes *B. burgdorferi* mammalian infectivity.

Spirochetes lacking *bb0318* exhibit reduced bacterial loads in mouse heart tissue. To further elucidate the infection phenotype of Δ*bb0318* spirochetes, we quantitated the spirochete loads in tissues from groups of six mice inoculated with wild-type, Δ*bb0318*/pBSV2G, or Δ*bb0318*/pBSV2G *bb0318* spirochetes at a dose of 1 × 10⁷, the dose at which Δ*bb0318*/pBSV2G spirochetes

are expected to infect the majority of mice tested (Table 2). All six mice inoculated with either wild-type or Δ*bb0318*/pBSV2G *bb0318* spirochetes were positive for infection as determined by reisolation of spirochetes from tissues and the presence of *B. burgdorferi*-specific antibodies (Table 3). Five of the six mice inoculated with Δ*bb0318*/pBSV2G spirochetes were positive for infection by the same qualitative measures (Table 3). Total DNA was extracted from ear, heart, and joint tissues of the infected mice. Quantitative PCR (qPCR) performed using DNA from each tissue as the template measured the number of *B. burgdorferi* genomes, represented by *flaB* copies, and the number of mouse genomes, represented by *nid* copies. Interestingly, the average spirochete load quantified from heart tissues of mice infected with Δ*bb0318* spirochetes was significantly lower than those of mice infected with spirochetes containing *bb0318* (Fig. 4A). In contrast, there was no significant difference in average spirochete loads measured in infected ear or joint tissues among all three clones (Fig. 4B and C). These data indicate not only that *bb0318* may be necessary for *B. burgdorferi* to achieve a wild-type infectious dose but also that spirochetes lacking *bb0318* may be dysfunctional in their ability to disseminate to and/or persist in the heart.

Spirochetes lacking *bb0318* demonstrate delayed infection kinetics in mice. As a means for gaining a better understanding of the possible dissemination defect of the Δ*bb0318* mutant clone, we performed a time course infection experiment. Groups of six mice each were infected with either wild-type, Δ*bb0318*/pBSV2G, or Δ*bb0318*/pBSV2G *bb0318* spirochetes at a dose of 1 × 10⁷. At 1 week, 2 weeks, and 3 weeks postinoculation, groups of mice were assessed for infection by reisolation of spirochetes from tissues, followed by quantitation of spirochete loads in tissues. *B. burgdorferi* lacking *bb0318* exhibited a marked delay in infection kinetics. Although 3 out of 6 mice were found to be infected with the mu-

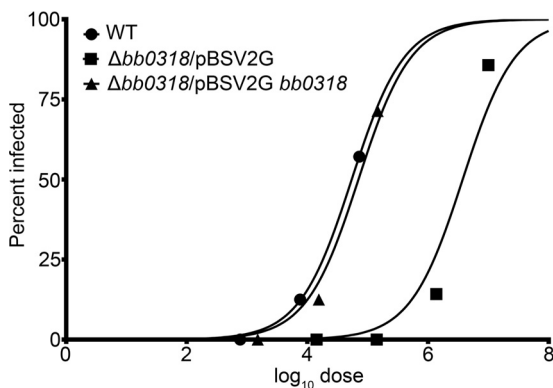


FIG 3 The 50% infectious dose (ID₅₀) of Δ*bb0318* spirochetes is 100-fold greater than those of wild-type and *bb0318*⁺ spirochetes. Groups of mice were inoculated intraperitoneally with various doses of wild-type (WT), Δ*bb0318*/pBSV2G, or Δ*bb0318*/pBSV2G *bb0318* spirochetes. Three weeks postinoculation, positive infection was determined based on spirochete reisolation from ear, bladder, and/or joint tissues. A mouse was considered infected if spirochetes were reisolated from at least one of the three tissues analyzed. The mouse infection data are presented in Table 3. Probit regression was used to plot the percentage of infected animals per group against the base 10 logarithm of the inoculum dose (log₁₀ dose).

TABLE 3 *B. burgdorferi* lacking *bb0318* displays qualitative measures of infection at a dose of 1 × 10⁷ spirochetes

Clone genotype	No. of positive mice/no. of mice analyzed as determined by:	Reisolation of spirochetes from tissues ^b		
		Serology ^a	Ear	Bladder
Wild type	6/6	6/6	6/6	6/6
Δ <i>bb0318</i> /pBSV2G	5/6	4/6	4/6	5/6
Δ <i>bb0318</i> /pBSV2G <i>bb0318</i>	6/6	5/6	6/6	6/6

^a Determined 3 weeks postinoculation by serological response to *B. burgdorferi* proteins.

^b Assessed 3 weeks postinoculation. A mouse was considered infected if spirochetes were reisolated from at least one of the three tissues analyzed.

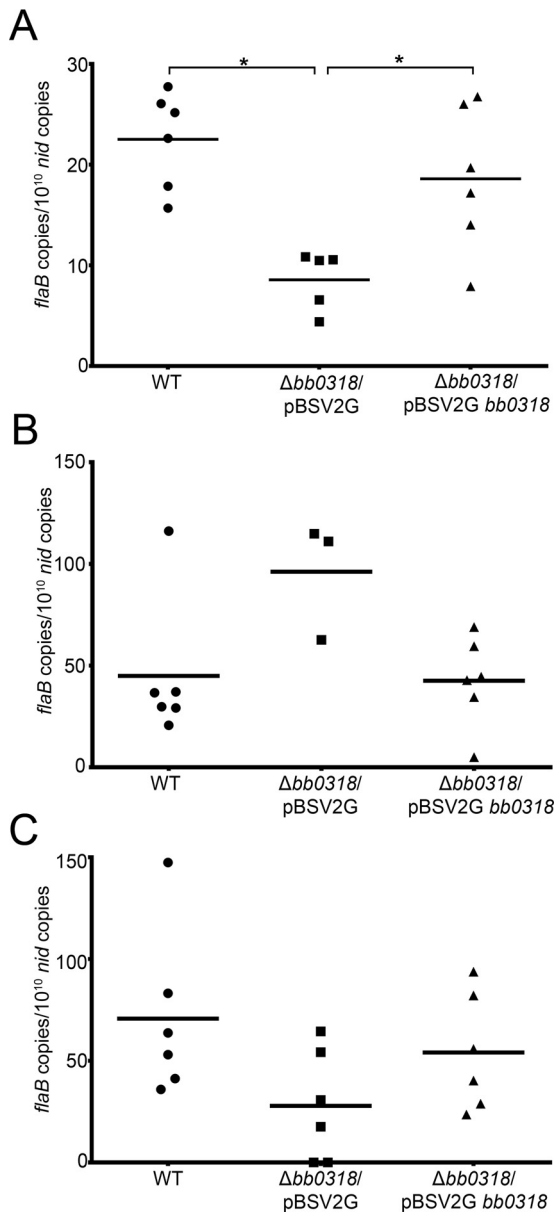


FIG 4 Spirochetes lacking *bb0318* exhibit reduced loads in heart tissue. Total DNA was isolated from spirochete-infected heart (A), ear (B), and joint (C) tissues harvested 3 weeks following the inoculation of mice with 1×10^7 wild-type (WT), $\Delta bb0318/pBSV2G$, or $\Delta bb0318/pBSV2G bb0318$ spirochetes. Spirochete loads in tissues were quantified by qPCR, and the data are presented as the number of spirochete *flaB* copies per 10^{10} mouse *nid* copies. The mean for each group of data is represented by a horizontal line. Data sets were compared across clones by use of one-way ANOVA and Tukey's posttest (GraphPad Prism, version 6.0). Statistical comparisons were not found to be significant unless otherwise noted. Asterisks indicate significant differences ($P < 0.05$).

tant at week 1 as defined by reisolation of spirochetes from at least one tissue, spirochetes were reisolated from only 17% of the ear and bladder tissues and 33% of the joint tissues (Fig. 5A). In contrast, at the same time point, spirochetes were reisolated from 100% of all tissues analyzed for mice inoculated with wild-type spirochetes and from 50% of the ear tissues and 67% of the bladder and joint tissues for mice inoculated with $\Delta bb0318/pBSV2G$

bb0318 spirochetes (Fig. 5A). Quantitative analysis of the spirochete loads in the ear, heart, and joint tissues of infected mice revealed the bacterial burdens of the $\Delta bb0318$ mutant and *bb0318* complement clones in the ear tissues to be significantly lower than that of the wild-type clone at week 1 (Fig. 5B). Overall, little infection was detected in the heart and joint tissues for all clones at this early time point, resulting in no significant clone-specific differences in spirochete loads (Fig. 5B). The $\Delta bb0318/pBSV2G$ spirochetes continued to demonstrate delayed dissemination to distal tissues at weeks 2 and 3 postinfection, with 50% and 83% of ear tissues and 33% and 67% of bladder and joint tissues positive for spirochete reisolation at the two time points, respectively (Fig. 5A). In contrast, wild-type and $\Delta bb0318/pBSV2G bb0318$ spirochetes were reisolated from 100% of the tissues analyzed at both weeks 2 and 3 (Fig. 5A). As was described for week 1, the bacterial burden of the $\Delta bb0318$ mutant in the ear tissues 2 weeks postinfection was significantly lower than that of the wild-type clone (Fig. 5C). There were no significant clone-specific differences between the spirochete loads in heart tissues at week 2, although the spirochete loads in the hearts at this time point suggested lower numbers of $\Delta bb0318$ spirochetes than of the clones carrying the *bb0318* gene (Fig. 5C). The joint tissues from mice infected with the *bb0318* complemented clone had bacterial burdens significantly different from the joint tissues of wild-type-infected mice at week 2, whereas the $\Delta bb0318$ clone-infected joints did not. By week 3, while the majority of mice inoculated with $\Delta bb0318$ spirochetes were positive for infection by reisolation (Fig. 5A), the spirochete loads measured in the heart tissues infected with the mutant were significantly lower than those for the wild-type and complemented clones, recapitulating the results shown in Fig. 4 (Fig. 5D). Together, these data indicate that spirochetes lacking *bb0318* are attenuated in their ability to disseminate early during infection and are unable to establish an infection in heart tissue through 3 weeks postinfection.

DISCUSSION

The nutrient salvage mechanisms that *B. burgdorferi* uses to survive during mammalian infection remain largely unknown but may represent novel targets for therapeutic intervention for Lyme disease. Using an *in vivo* expression technology (IVET)-based approach to screen for *B. burgdorferi* genes expressed during an active murine infection, we previously identified gene *bb0318* (28), which is predicted to encode the ATPase component of a putative riboflavin ABC transport system (1, 29). We have now demonstrated that *bb0318* contributes to the ability of *B. burgdorferi* to survive in the presence of oxidative stress and is important for mammalian infection.

Without the ATPase to hydrolyze ATP and drive the activity of the transport system, the functionality of an ABC transporter is either significantly reduced or eliminated (48, 49). By deleting *bb0318*, the gene encoding the ATPase of a putative riboflavin transport system, we investigated the effects of removing the functionality of the transport system on *B. burgdorferi* biology both *in vitro* and *in vivo*. The *bb0318* gene was found to be dispensable for growth under standard *in vitro* conditions, indicating that the gene does not provide an essential function in nutrient-rich growth medium. The transport system encoded by *bb0319* to *bb0316* has been proposed to take up riboflavin (29), and riboflavin is the precursor for the synthesis of cofactors FMN and FAD, which are critical for the CoA/CoADR redox system, leading to

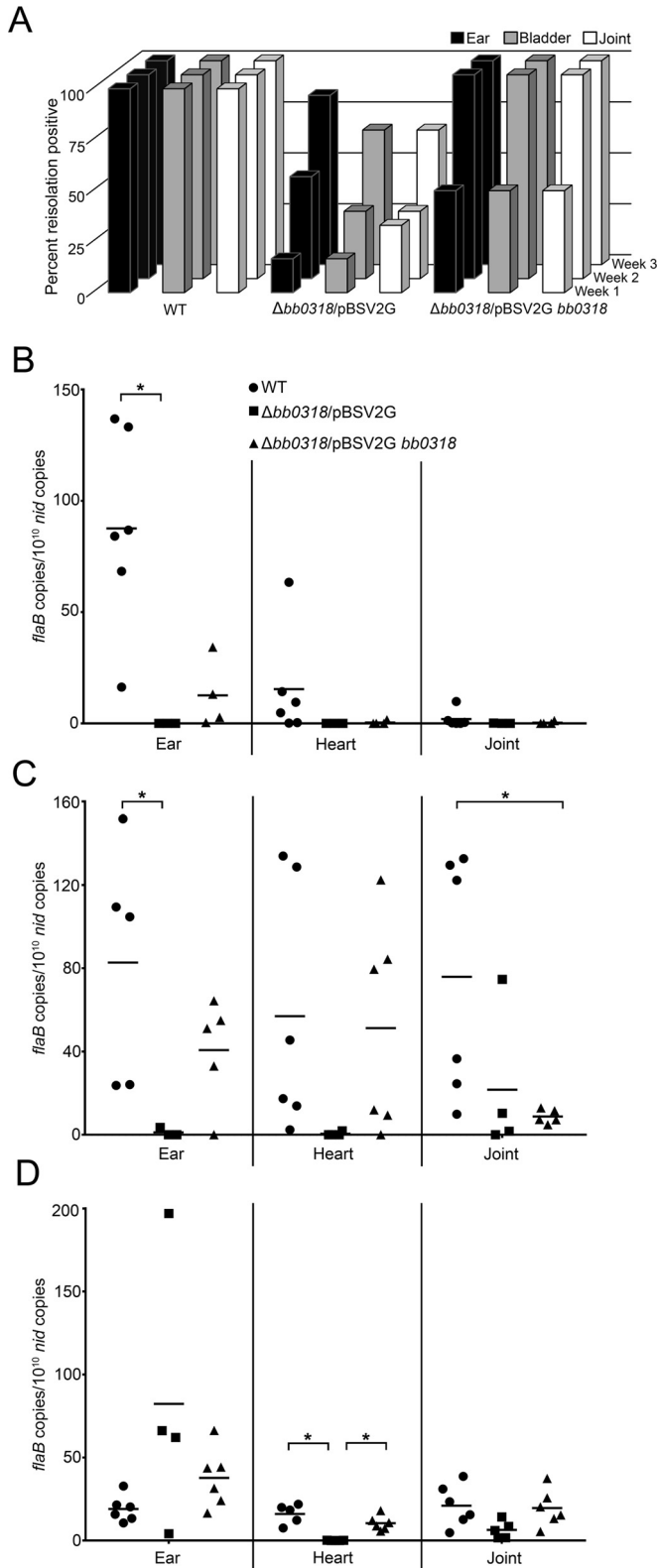


FIG 5 Spirochetes lacking *bb0318* demonstrate delayed infection kinetics. Groups of mice were needle inoculated with 1×10^7 wild-type (WT), $\Delta bb0318/pBSV2G$, or $\Delta bb0318/pBSV2G bb0318$ spirochetes. (A) At 1, 2, or 3 weeks postinoculation, mice were analyzed for infection by reisolation of spirochetes from ear, bladder, and joint tissues. Data are represented as the percentage of each tissue type from each group of mice found to be positive for

our hypothesis that *bb0318* may contribute to the resistance of *B. burgdorferi* to oxidative stress. In agreement with this hypothesis, we demonstrated that spirochetes lacking *bb0318* had a diminished ability to survive in the presence of high concentrations of H_2O_2 under microaerobic growth conditions and when challenged with murine macrophages. This phenotype is similar to what has been reported for spirochetes lacking the ROS scavenger superoxide dismutase when they are challenged with both chemical and biological sources of oxidative stress (14).

Previous work examining *B. burgdorferi* lacking CoADR determined that CoADR plays a role in the oxidative stress response by mediating the CoA/CoASH thiol redox system (11). Although this enzyme was proposed to protect the spirochete against H_2O_2 , the *cdr* mutant was found not to differ significantly from wild-type *B. burgdorferi* in sensitivity to H_2O_2 stress (11, 13). However, this system may not be the only small-thiol redox system in *B. burgdorferi*; its genome contains genes encoding thioredoxin (*trxA*; *bb0061*) and thioredoxin reductase (*trxB*; *bb0515*) (9, 13), which may represent an additional active redox system. Because both CoA and thioredoxin reductases use FAD to reduce their respective small thiols (13, 50), the lack of sensitivity of the Δcdr mutant to H_2O_2 may be due to compensation by the alternative redox system. In contrast, spirochetes lacking *bb0318* may be unable to acquire sufficient riboflavin, necessary for FAD synthesis, for the function of both redox systems. Alternatively, our data do not rule out the possibility that *bb0318* contributes another, yet-to-be-determined function to *B. burgdorferi* biology.

A link between riboflavin uptake and oxidative stress resistance has been demonstrated for other bacterial species. *Lactococcus lactis* exhibits heat-induced sensitivity to oxidative stress from dissolved oxygen in the growth medium and a temperature-dependent decrease in intracellular FAD levels. This phenotype could be rescued by overexpression of a riboflavin transporter, leading to restored FAD biosynthesis and bacterial fitness (51). As *B. burgdorferi* enters the bloodstream to disseminate to deep tissues, it encounters an oxidative environment due to the dissolved oxygen present in the blood. As with *L. lactis*, survival under these conditions may depend on the spirochete's ability to salvage riboflavin for sufficient FAD biosynthesis and oxidative stress resistance. Similarly, *B. burgdorferi* may encounter deleterious reactive oxygen species during the tick stages of the infectious cycle. Indeed, the BosR-regulated putative oxidative stress gene *bb0690* (*napA*; *dps*) is critical for spirochete persistence in unfed ticks (52), and CoADR contributes to survival in feeding ticks (13). We found that the expression of *bb0318*, along with that of *bb0319*, *bb0317*, and *bb0316*, was higher in unfed nymphs than in fed nymphs and mouse tissues, suggesting that in addition to the role of *bb0318* in the mouse, this gene, and likely genes *bb0319* to *bb0316*, may also contribute to *B. burgdorferi* survival in the tick.

spirochete reisolation at each time point. (B through D) DNA was isolated only from the tissues of those mice found to be positive for infection, as defined by reisolation of spirochetes from at least one of the three tissues analyzed, at week 1 (B), week 2 (C), and week 3 (D) postinoculation. All DNA was measured by qPCR in triplicate for spirochete loads, and data are presented as the number of spirochete *flaB* copies per 10^{10} mouse *nid* copies. The mean for each group of data is represented by a horizontal line. Data were compared using one-way ANOVA and Tukey's posttest (GraphPad Prism, version 6.0). Statistical comparisons were not found to be significant unless otherwise noted. Asterisks indicate significant differences ($P < 0.05$).

B. burgdorferi has been shown to undergo a population bottleneck upon inoculation into the mammalian host (53, 54). The innate immune response is critical for controlling *B. burgdorferi* infection (55–58). The magnitude of the spirochete population bottleneck has been shown to be reduced in mice with an impaired innate immune system (54). The oxidative stress that the spirochete encounters during the initial stages of mammalian infection may be due to H₂O₂ production by innate immune cells, such as macrophages and neutrophils, during the host inflammatory response (9). Our data indicate that *B. burgdorferi* lacking *bb0318* has increased susceptibility to killing by murine macrophages *in vitro*, suggesting that this mutant may be particularly vulnerable to the bottleneck effect of the host innate immune response early in mammalian infection, resulting in an attenuation in virulence. The 50% infectious dose of the *bb0318* mutant was found to be 100-fold higher than that of spirochetes harboring *bb0318*. The infectivity defect of spirochetes lacking *bb0318* is consistent with what has been reported for this gene in both a genomewide signature-tagged mutagenesis study and an analysis of *B. burgdorferi* genes important for pathogenesis that combined transposon mutagenesis with high-throughput sequencing (Tn-seq) (59–61). Because *B. burgdorferi* lacking *bb0318* was able to infect mice at a dose of 1×10^7 spirochetes, we were able to gain insight into the requirement of *B. burgdorferi* for *bb0318* in order to infect mice. At a high-dose inoculum, Δ *bb0318* spirochetes were defective in their ability to disseminate early during infection; they did not reach wild-type levels of reisolation-positive tissues until 3 weeks post-inoculation. Moreover, even at 3 weeks postinoculation, spirochetes were not detected in the heart tissues of mice infected with the Δ *bb0318* clone. These data suggest that at a high-dose inoculum, the Δ *bb0318* mutant is able to partially overcome its virulence defect. Despite the increased susceptibility of spirochetes lacking *bb0318* to macrophage killing, at the dose of 1×10^7 spirochetes, the Δ *bb0318* mutant may be able to overwhelm the innate immune system, allowing some fraction of the spirochete population to escape and cause a disseminated infection, though to a lesser extent than wild-type spirochetes. In addition, it is possible that at this dose, the high density of spirochetes offers a protective effect against the innate immune system, resulting from the action of ROS detoxification proteins that do not rely on riboflavin to generate the FAD cofactor, such as the superoxide dismutase activity of SodA (14, 26, 27, 62) and/or additional, yet-to-be-defined BosR-regulated proteins (24). It is noteworthy that although a number of putative mechanisms may compensate for the pathogenesis defects of the Δ *bb0318* spirochetes, none allowed the mutant to infect the heart tissue, suggesting that this mutant may provide insight into the molecular mechanisms of *B. burgdorferi* colonization of the heart. Taken together, these findings suggest that the *bb0318* gene, and therefore the BB0319-to-BB0316 transport system, may be critical for the ability of *B. burgdorferi* to resist killing by the oxidative stress conditions produced by innate immune cells and signaling molecules early during infection, as well as for the ability of *B. burgdorferi* to disseminate to the heart.

In this study, we demonstrated that as the gene encoding the ATPase of a putative transport system, *bb0318* is necessary for *B. burgdorferi* to maintain a wild-type infection in mice, not only with regard to the number of spirochetes required to mount an infection but also with regard to the ability to disseminate effectively. Furthermore, we give evidence that Δ *bb0318* spirochetes are more susceptible than wild-type or complemented spirochetes

to oxidative stress from H₂O₂, as well as to murine macrophages *in vitro*. Although much remains to be studied about the interplay of *B. burgdorferi* nutrient salvage and the oxidative stress response, and its meaning for the pathogen's survival throughout the infectious cycle, this work provides insight into the mechanisms by which the acquisition and use of metabolic precursors may contribute to *B. burgdorferi* pathogenesis in the mammalian host.

ACKNOWLEDGMENTS

Thank you to Frank Gherardini and Travis Bourret for insightful comments and suggestions. We are grateful to Kyle Rohde and Sandra Geden for providing the J774 macrophages. We appreciate all the invaluable technical and intellectual contributions of Travis Jewett. Thank you to Carlos Flores Avile for technical assistance. Thank you to the NAF animal care staff. The following reagent was provided by Centers for Disease Control and Prevention for distribution by BEI Resources, NIAID, NIH: *Ixodes scapularis* Larvae (Live), NR-44115.

FUNDING INFORMATION

This work was funded by National Research Fund for Tick-Borne Diseases (Pilot Grant 2012-2013 to M.W.J.) and the National Institute of Allergy and Infectious Diseases (NIAID) (R01AI099094 and K22AI081730 to M.W.J.).

REFERENCES

- Fraser CM, Casjens S, Huang WM, Sutton GG, Clayton R, Lathigra R, White O, Ketchum KA, Dodson R, Hickey EK, Gwinn M, Dougherty B, Tomb JF, Fleischmann RD, Richardson D, Peterson J, Kerlavage AR, Quackenbush J, Salzberg S, Hanson M, van Vugt R, Palmer N, Adams MD, Gocayne J, Weidman J, Utterback T, Wattney L, McDonald L, Artiach P, Bowman C, Garland S, Fuji C, Cotton MD, Horst K, Roberts K, Hatch B, Smith HO, Venter JC. 1997. Genomic sequence of a Lyme disease spirochaete, *Borrelia burgdorferi*. *Nature* 390:580–586. <http://dx.doi.org/10.1038/37551>.
- Brisson D, Zhou W, Jutras BL, Casjens S, Stevenson B. 2013. Distribution of cp32 prophages among Lyme disease-causing spirochetes and natural diversity of their lipoprotein-encoding *erp* loci. *Appl Environ Microbiol* 79:4115–4128. <http://dx.doi.org/10.1128/AEM.00817-13>.
- Casjens S, Palmer N, van Vugt R, Huang WM, Stevenson B, Rosa P, Lathigra R, Sutton G, Peterson J, Dodson RJ, Haft D, Hickey E, Gwinn M, White O, Fraser CM. 2000. A bacterial genome in flux: the twelve linear and nine circular extrachromosomal DNAs in an infectious isolate of the Lyme disease spirochete *Borrelia burgdorferi*. *Mol Microbiol* 35:490–516. <http://dx.doi.org/10.1046/j.1365-2958.2000.01698.x>.
- Saier MH, Jr, Paulsen IT. 2000. Whole genome analyses of transporters in spirochetes: *Borrelia burgdorferi* and *Treponema pallidum*. *J Mol Microbiol Biotechnol* 2:393–399.
- Jain S, Showman AC, Jewett MW. 2015. Molecular dissection of a *Borrelia burgdorferi* *in vivo* essential purine transport system. *Infect Immun* 83:2224–2233. <http://dx.doi.org/10.1128/IAI.02859-14>.
- Jain S, Sutchu S, Rosa PA, Byram R, Jewett MW. 2012. *Borrelia burgdorferi* harbors a transport system essential for purine salvage and mammalian infection. *Infect Immun* 80:3086–3093. <http://dx.doi.org/10.1128/IAI.00514-12>.
- Khajanchi BK, Odeh E, Gao L, Jacobs MB, Philipp MT, Lin T, Norris SJ. 2016. Phosphoenolpyruvate phosphotransferase system components modulate gene transcription and virulence of *Borrelia burgdorferi*. *Infect Immun* 84:754–764. <http://dx.doi.org/10.1128/IAI.00917-15>.
- Ouyang Z, He M, Oman T, Yang XF, Norgard MV. 2009. A manganese transporter, BB0219 (BmtA), is required for virulence by the Lyme disease spirochete, *Borrelia burgdorferi*. *Proc Natl Acad Sci U S A* 106:3449–3454. <http://dx.doi.org/10.1073/pnas.0812999106>.
- Boylan JA, Gherardini FC. 2008. Determining the cellular targets of reactive oxygen species in *Borrelia burgdorferi*. *Methods Mol Biol* 431:213–221.
- Posey JE, Gherardini FC. 2000. Lack of a role for iron in the Lyme disease pathogen. *Science* 288:1651–1653. <http://dx.doi.org/10.1126/science.288.5471.1651>.
- Boylan JA, Hummel CS, Benoit S, Garcia-Lara J, Treglown-Downey J,

- Crane EJ, III, Gherardini FC. 2006. *Borrelia burgdorferi* bb0728 encodes a coenzyme A disulphide reductase whose function suggests a role in intracellular redox and the oxidative stress response. *Mol Microbiol* 59:475–486. <http://dx.doi.org/10.1111/j.1365-2958.2005.04963.x>.
12. Boylan JA, Posey JE, Gherardini FC. 2003. *Borrelia* oxidative stress response regulator, BosR: a distinctive Zn-dependent transcriptional activator. *Proc Natl Acad Sci U S A* 100:11684–11689. <http://dx.doi.org/10.1073/pnas.2032956100>.
 13. Eggers CH, Caimano MJ, Malizia RA, Kariu T, Cusack B, Desrosiers DC, Hazlett KR, Claiborne A, Pal U, Radolf JD. 2011. The coenzyme A disulphide reductase of *Borrelia burgdorferi* is important for rapid growth throughout the enzootic cycle and essential for infection of the mammalian host. *Mol Microbiol* 82:679–697. <http://dx.doi.org/10.1111/j.1365-2958.2011.07845.x>.
 14. Esteve-Gassent MD, Elliott NL, Seshu J. 2009. *sodA* is essential for virulence of *Borrelia burgdorferi* in the murine model of Lyme disease. *Mol Microbiol* 71:594–612. <http://dx.doi.org/10.1111/j.1365-2958.2008.06549.x>.
 15. Narasimhan S, Sukumaran B, Bozdogan U, Thomas V, Liang X, DePonte K, Marcantonio N, Koski RA, Anderson JF, Kantor F, Fikrig E. 2007. A tick antioxidant facilitates the Lyme disease agent's successful migration from the mammalian host to the arthropod vector. *Cell Host Microbe* 2:7–18. <http://dx.doi.org/10.1016/j.chom.2007.06.001>.
 16. Seshu J, Boylan JA, Gherardini FC, Skare JT. 2004. Dissolved oxygen levels alter gene expression and antigen profiles in *Borrelia burgdorferi*. *Infect Immun* 72:1580–1586. <http://dx.doi.org/10.1128/IAI.72.3.1580-1586.2004>.
 17. Seshu J, Boylan JA, Hyde JA, Swingle KL, Gherardini FC, Skare JT. 2004. A conservative amino acid change alters the function of BosR, the redox regulator of *Borrelia burgdorferi*. *Mol Microbiol* 54:1352–1363. <http://dx.doi.org/10.1111/j.1365-2958.2004.04352.x>.
 18. Katona LI. 2015. The Fur homologue BosR requires Arg39 to activate *rpoS* transcription in *Borrelia burgdorferi* and thereby direct spirochaete infection in mice. *Microbiology* 161:2243–2255. <http://dx.doi.org/10.1099/mic.0.000166>.
 19. Ouyang Z, Deka RK, Norgard MV. 2011. BosR (BB0647) controls the RpoN-RpoS regulatory pathway and virulence expression in *Borrelia burgdorferi* by a novel DNA-binding mechanism. *PLoS Pathog* 7:e1001272. <http://dx.doi.org/10.1371/journal.ppat.1001272>.
 20. Ouyang Z, Kumar M, Kariu T, Haq S, Goldberg M, Pal U, Norgard MV. 2009. BosR (BB0647) governs virulence expression in *Borrelia burgdorferi*. *Mol Microbiol* 74:1331–1343. <http://dx.doi.org/10.1111/j.1365-2958.2009.06945.x>.
 21. Ouyang Z, Zhou J, Norgard MV. 2016. Evidence that BosR (BB0647) is a positive autoregulator in *Borrelia burgdorferi*. *Infect Immun* 84:2566–2574. <http://dx.doi.org/10.1128/IAI.00297-16>.
 22. Shi Y, Dadhwal P, Li X, Liang FT. 2014. BosR functions as a repressor of the *ospAB* operon in *Borrelia burgdorferi*. *PLoS One* 9:e109307. <http://dx.doi.org/10.1371/journal.pone.0109307>.
 23. Wang P, Dadhwal P, Cheng Z, Zianni MR, Rikihisa Y, Liang FT, Li X. 2013. *Borrelia burgdorferi* oxidative stress regulator BosR directly represses lipoproteins primarily expressed in the tick during mammalian infection. *Mol Microbiol* 89:1140–1153. <http://dx.doi.org/10.1111/mmi.12337>.
 24. Hyde JA, Seshu J, Skare JT. 2006. Transcriptional profiling of *Borrelia burgdorferi* containing a unique *bosR* allele identifies a putative oxidative stress regulon. *Microbiology* 152:2599–2609. <http://dx.doi.org/10.1099/mic.0.28996-0>.
 25. Hyde JA, Shaw DK, Smith R, III, Trzeciakowski JP, Skare JT. 2009. The BosR regulatory protein of *Borrelia burgdorferi* interfaces with the RpoS regulatory pathway and modulates both the oxidative stress response and pathogenic properties of the Lyme disease spirochete. *Mol Microbiol* 74:1344–1355. <http://dx.doi.org/10.1111/j.1365-2958.2009.06951.x>.
 26. Troxell B, Xu H, Yang XF. 2012. *Borrelia burgdorferi*, a pathogen that lacks iron, encodes manganese-dependent superoxide dismutase essential for resistance to streptonigrin. *J Biol Chem* 287:19284–19293. <http://dx.doi.org/10.1074/jbc.M112.344903>.
 27. Esteve-Gassent MD, Smith TC, II, Small CM, Thomas DP, Seshu J. 2015. Absence of *sodA* increases the levels of oxidation of key metabolic determinants of *Borrelia burgdorferi*. *PLoS One* 10:e0136707. <http://dx.doi.org/10.1371/journal.pone.0136707>.
 28. Ellis TC, Jain S, Linowski AK, Rike K, Bestor A, Rosa PA, Halpern M, Kurhanewicz S, Jewett MW. 2013. *In vivo* expression technology identifies a novel virulence factor critical for *Borrelia burgdorferi* persistence in mice. *PLoS Pathog* 9:e1003567. <http://dx.doi.org/10.1371/journal.ppat.1003567>. (Erratum, 10:e1004260, 2014, <http://dx.doi.org/10.1371/journal.ppat.1004260>.)
 29. Deka RK, Brautigam CA, Biddy BA, Liu WZ, Norgard MV. 2013. Evidence for an ABC-type riboflavin transporter system in pathogenic spirochetes. *mBio* 4(1):e00615-12. <http://dx.doi.org/10.1128/mBio.00615-12>.
 30. Dam P, Olman V, Harris K, Su Z, Xu Y. 2007. Operon prediction using both genome-specific and general genomic information. *Nucleic Acids Res* 35:288–298. <http://dx.doi.org/10.1093/nar/gkl1018>.
 31. Mao F, Dam P, Chou J, Olman V, Xu Y. 2009. DOOR: a database for prokaryotic operons. *Nucleic Acids Res* 37:D459–D463. <http://dx.doi.org/10.1093/nar/gkn757>.
 32. Serrano A, Ferreira P, Martinez-Julvez M, Medina M. 2013. The prokaryotic FAD synthetase family: a potential drug target. *Curr Pharm Des* 19:2637–2648. <http://dx.doi.org/10.2174/1381612811319140013>.
 33. Gherardini F, Boylan J, Lawrence K, Skare J. 2010. Metabolism and physiology of *Borrelia*, p 103–138. In Samuels DS, Radolf JD (ed), *Borrelia*: molecular biology, host interaction and pathogenesis. Caister Academic Press, Norfolk, United Kingdom.
 34. Marchler-Bauer A, Derbyshire MK, Gonzales NR, Lu S, Chitsaz F, Geer LY, Geer RC, He J, Gwadz M, Hurwitz DI, Lanczycki CJ, Lu F, Marchler GH, Song JS, Thanki N, Wang Z, Yamashita RA, Zhang D, Zheng C, Bryant SH. 2015. CDD: NCBI's conserved domain database. *Nucleic Acids Res* 43:D222–D226. <http://dx.doi.org/10.1093/nar/gku1221>.
 35. Rego RO, Bestor A, Rosa PA. 2011. Defining the plasmid-borne restriction-modification systems of the Lyme disease spirochete *Borrelia burgdorferi*. *J Bacteriol* 193:1161–1171. <http://dx.doi.org/10.1128/JB.01176-10>.
 36. Rosa PA, Hogan D. 1992. Colony formation by *Borrelia burgdorferi* in solid medium: clonal analysis of *osp* locus variants, p 95–103. In Munderloh UG, Kurtti TJ (ed), First International Conference on Tick Borne Pathogens at the Host-Vector Interface; an agenda for research: proceedings and abstracts, September 15–18, 1992. University of Minnesota, St. Paul, MN.
 37. Samuels DS. 1995. Electrotransformation of the spirochete *Borrelia burgdorferi*. *Methods Mol Biol* 47:253–259.
 38. Jewett MW, Lawrence K, Bestor AC, Tilly K, Grimm D, Shaw P, VanRaden M, Gherardini F, Rosa PA. 2007. The critical role of the linear plasmid lp36 in the infectious cycle of *Borrelia burgdorferi*. *Mol Microbiol* 64:1358–1374. <http://dx.doi.org/10.1111/j.1365-2958.2007.05746.x>.
 39. Elias AF, Stewart PE, Grimm D, Caimano MJ, Eggers CH, Tilly K, Bono JL, Akins DR, Radolf JD, Schwan TG, Rosa P. 2002. Clonal polymorphism of *Borrelia burgdorferi* strain B31 MI: implications for mutagenesis in an infectious strain background. *Infect Immun* 70:2139–2150. <http://dx.doi.org/10.1128/IAI.70.4.2139-2150.2002>.
 40. Elias AF, Bono JL, Kupko JJ, III, Stewart PE, Krum JG, Rosa PA. 2003. New antibiotic resistance cassettes suitable for genetic studies in *Borrelia burgdorferi*. *J Mol Microbiol Biotechnol* 6:29–40. <http://dx.doi.org/10.1159/000073406>.
 41. Drecktrah D, Lybecker M, Popitsch N, Rescheneder P, Hall LS, Samuels DS. 2015. The *Borrelia burgdorferi* RelA/SpoT homolog and stringent response regulate survival in the tick vector and global gene expression during starvation. *PLoS Pathog* 11:e1005160. <http://dx.doi.org/10.1371/journal.ppat.1005160>.
 42. Troxell B, Zhang JJ, Bourret TJ, Zeng MY, Blum J, Gherardini F, Hassan HM, Yang XF. 2014. Pyruvate protects pathogenic spirochetes from H₂O₂ killing. *PLoS One* 9:e84625. <http://dx.doi.org/10.1371/journal.pone.0084625>.
 43. Jewett MW, Lawrence KA, Bestor A, Byram R, Gherardini F, Rosa PA. 2009. GuaA and GuaB are essential for *Borrelia burgdorferi* survival in the tick-mouse infection cycle. *J Bacteriol* 191:6231–6241. <http://dx.doi.org/10.1128/JB.00450-09>.
 44. Jewett MW, Byram R, Bestor A, Tilly K, Lawrence K, Burtnick MN, Gherardini F, Rosa PA. 2007. Genetic basis for retention of a critical virulence plasmid of *Borrelia burgdorferi*. *Mol Microbiol* 66:975–990. <http://dx.doi.org/10.1111/j.1365-2958.2007.05969.x>.
 45. Modolell M, Schaible UE, Rittig M, Simon MM. 1994. Killing of *Borrelia burgdorferi* by macrophages is dependent on oxygen radicals and nitric oxide and can be enhanced by antibodies to outer surface proteins of the spirochete. *Immunol Lett* 40:139–146. [http://dx.doi.org/10.1016/0165-2478\(94\)90185-6](http://dx.doi.org/10.1016/0165-2478(94)90185-6).
 46. Bestor A, Rego RO, Tilly K, Rosa PA. 2012. Competitive advantage of *Borrelia burgdorferi* with outer surface protein BBA03 during tick-

- mediated infection of the mammalian host. *Infect Immun* 80:3501–3511. <http://dx.doi.org/10.1128/IAI.00521-12>.
47. Moon KH, Hobbs G, Motaleb MA. 2016. *Borrelia burgdorferi* CheD promotes various functions in chemotaxis and the pathogenic life cycle of the spirochete. *Infect Immun* 84:1743–1752. <http://dx.doi.org/10.1128/IAI.01347-15>.
 48. Davidson AL, Sharma S. 1997. Mutation of a single MalK subunit severely impairs maltose transport activity in *Escherichia coli*. *J Bacteriol* 179:5458–5464.
 49. Liu CE, Liu PQ, Ames GF. 1997. Characterization of the adenosine triphosphatase activity of the periplasmic histidine permease, a traffic ATPase (ABC transporter). *J Biol Chem* 272:21883–21891. <http://dx.doi.org/10.1074/jbc.272.35.21883>.
 50. Lu J, Holmgren A. 2014. The thioredoxin antioxidant system. *Free Radic Biol Med* 66:75–87. <http://dx.doi.org/10.1016/j.freeradbiomed.2013.07.036>.
 51. Chen J, Shen J, Solem C, Jensen PR. 2013. Oxidative stress at high temperatures in *Lactococcus lactis* due to an insufficient supply of riboflavin. *Appl Environ Microbiol* 79:6140–6147. <http://dx.doi.org/10.1128/AEM.01953-13>.
 52. Li X, Pal U, Ramamoorthi N, Liu X, Desrosiers DC, Eggers CH, Anderson JF, Radolf JD, Fikrig E. 2007. The Lyme disease agent *Borrelia burgdorferi* requires BB0690, a Dps homologue, to persist within ticks. *Mol Microbiol* 63:694–710. <http://dx.doi.org/10.1111/j.1365-2958.2006.05550.x>.
 53. Rego RO, Bestor A, Stefka J, Rosa PA. 2014. Population bottlenecks during the infectious cycle of the Lyme disease spirochete *Borrelia burgdorferi*. *PLoS One* 9:e101009. <http://dx.doi.org/10.1371/journal.pone.0101009>.
 54. Troy EB, Lin T, Gao L, Lazinski DW, Camilli A, Norris SJ, Hu L. 2013. Understanding barriers to *Borrelia burgdorferi* dissemination during infection using massively parallel sequencing. *Infect Immun* 81:2347–2357. <http://dx.doi.org/10.1128/IAI.00266-13>.
 55. Bockenstedt LK, Liu N, Schwartz I, Fish D. 2006. MyD88 deficiency enhances acquisition and transmission of *Borrelia burgdorferi* by *Ixodes scapularis* ticks. *Infect Immun* 74:2154–2160. <http://dx.doi.org/10.1128/IAI.74.4.2154-2160.2006>.
 56. Bolz DD, Sundsbak RS, Ma Y, Akira S, Kirschning CJ, Zachary JF, Weis JH, Weis JJ. 2004. MyD88 plays a unique role in host defense but not arthritis development in Lyme disease. *J Immunol* 173:2003–2010. <http://dx.doi.org/10.4049/jimmunol.173.3.2003>.
 57. Liu N, Montgomery RR, Barthold SW, Bockenstedt LK. 2004. Myeloid differentiation antigen 88 deficiency impairs pathogen clearance but does not alter inflammation in *Borrelia burgdorferi*-infected mice. *Infect Immun* 72:3195–3203. <http://dx.doi.org/10.1128/IAI.72.6.3195-3203.2004>.
 58. Petnicki-Ocwieja T, Kern A. 2014. Mechanisms of *Borrelia burgdorferi* internalization and intracellular innate immune signaling. *Front Cell Infect Microbiol* 4:175. <http://dx.doi.org/10.3389/fcimb.2014.00175>.
 59. Lin T, Gao L, Zhang C, Odeh E, Jacobs MB, Coutte L, Chaconas G, Philipp MT, Norris SJ. 2012. Analysis of an ordered, comprehensive STM mutant library in infectious *Borrelia burgdorferi*: insights into the genes required for mouse infectivity. *PLoS One* 7:e47532. <http://dx.doi.org/10.1371/journal.pone.0047532>.
 60. Lin T, Troy EB, Hu LT, Gao L, Norris SJ. 2014. Transposon mutagenesis as an approach to improved understanding of *Borrelia* pathogenesis and biology. *Front Cell Infect Microbiol* 4:63. <http://dx.doi.org/10.3389/fcimb.2014.00063>.
 61. Troy EB, Lin T, Gao L, Lazinski DW, Lundt M, Camilli A, Norris SJ, Hu LT. 9 June 2016. Global Tn-seq analysis of carbohydrate utilization and vertebrate infectivity of *Borrelia burgdorferi*. *Mol Microbiol*. <http://dx.doi.org/10.1111/mmi.13437>.
 62. Aguirre JD, Clark HM, McIlvin M, Vazquez C, Palmere SL, Grab DJ, Seshu J, Hart PJ, Saito M, Culotta VC. 2013. A manganese-rich environment supports superoxide dismutase activity in a Lyme disease pathogen, *Borrelia burgdorferi*. *J Biol Chem* 288:8468–8478. <http://dx.doi.org/10.1074/jbc.M112.433540>.